Available online at www.sciencedirect.com
ScienceDirect
Journal of Molecular Graphics and Modelling 26 (2008) 1237–1251
Journal of Molecular Graphics and Modelling
www.elsevier.com/locate/JMGM

# Is it possible to increase hit rates in structure-based virtual screening by pharmacophore filtering? An investigation of the advantages and pitfalls of post-filtering

Daniel Muthas, Yogesh A. Sabnis, Magnus Lundborg, Anders Karlén *

*Department of Medicinal Chemistry, Division of Organic Pharmaceutical Chemistry, BMC, Uppsala University, P.O. Box 574, SE-751 23 Uppsala, Sweden*

Received 20 June 2007; received in revised form 16 November 2007; accepted 21 November 2007
Available online 18 January 2008

**Abstract**

We have investigated the influence of post-filtering virtual screening results, with pharmacophoric features generated from an X-ray structure, on enrichment rates. This was performed using three docking softwares, zdock+, Surflex and FRED, as virtual screening tools and pharmacophores generated in UNITY from co-crystallized complexes. Sets of known actives along with 9997 pharmaceutically relevant decoy compounds were docked against six chemically diverse protein targets namely CDK2, COX2, ERα, fXa, MMP3, and NA. To try to overcome the inherent limitations of the well-known docking problem, we generated multiple poses for each compound. The compounds were first ranked according to their scores alone and enrichment rates were calculated using only the top scoring pose of each compound. Subsequently, all poses for each compound were passed through the different pharmacophores generated from co-crystallized complexes and the enrichment factors were re-calculated based on the top-scoring passing pose of each compound. Post-filtering with a pharmacophore generated from only one X-ray complex was shown to increase enrichment rates in all investigated targets compared to docking alone. This indicates that this is a general method, which works for diverse targets and different docking softwares.


*Keywords:* Flo+; Surflex; FRED; Enrichment factor; Docking performance; Structure-based virtual screening; Pharmacophore filtering

## 1. Introduction

It is estimated that bringing a drug from idea to market takes approximately 12 years and costs as much as US$ 802 millions [1]. To cope with this high cost, more cost-efficient methods are required and various experimental and theoretical approaches have been developed. Virtual screening (VS) has arisen as an efficient method for rapidly identifying hits in terms of cost and time [2]. When the 3D-structure of the target is known, either by experimental or computational techniques, virtual screening is often performed by using structure-based docking [3]. With the advent of novel algorithms and faster computers it is now possible to screen millions of compounds in a matter of days. Virtual screening methods have been validated for their performance in several different studies (see for example Refs. [4–16]) and although these methods have been successfully used, they have some inherent limitations.

The so-called *docking problem* consists of correctly identifying the binding mode of a compound, i.e. finding the correct conformation and placement within the active site. The success of a docking is often compromised by the fact that the associated scoring functions often cannot resolve the most likely binding mode [17]. This highlights the importance of inspecting multiple conformations for the docked compounds and not only the highest scoring one. However, one can only visually inspect a much smaller number of compounds than the number of compounds usually contained in a screening library [18].

Database searching based on pharmacophore constraints is an alternative VS strategy [19–23]. One advantage of using pharmacophores is that they focus on specific key interactions for protein ligand binding. However, this approach does not perform optimally when used alone since little or no consideration of the shape of the binding site is taken into

* Corresponding author at: Department of Medicinal Chemistry, Uppsala University, Box 574, SE-751 23 Uppsala, Sweden. Tel.: +46 18 471 4293; fax: +46 18 471 4474.
*E-mail address:* anders.karlen@orgfarm.uu.se (A. Karlén).

1093-3263/$ – see front matter © 2007 Elsevier Inc. All rights reserved.
doi:10.1016/j.jmgm.2007.11.005

account. Therefore, it is useful to have methods that make optimal use of both docking and pharmacophores to improve the selection of active molecules [21,24–28].

Docking and pharmacophores can be linked in different ways, e.g. by incorporating a pharmacophore constraint into the docking scheme, or by using pharmacophores as a post-filter of unconstrained docking poses [29]. A possible limitation with the introduction of pharmacophore constraints during the docking process is that if the specified features have to be adjusted, the docking has to be re-performed. In contrast, if the pharmacophore post-filtering approach is used, the features can easily be adjusted without re-performing the more time-consuming docking step. An additional benefit with pharmacophore post-filters is that they can easily be applied to results from any docking software.

The aim of this study is to combine the docking and pharmacophore-based approach in VS and to investigate the enrichment obtained after pharmacophoric post-filtering of docked poses and compared it to that after docking alone. We were interested to see if very limited prior information (one co-complexed ligand) could aid in identifying intrinsic binding features, and thereby help to retrieve a larger fraction of active molecules. The experiments were setup to simulate the situation faced by computational medicinal chemists early in a project where limited information about target–ligand interactions is known. To assess the generality of the approach we employed three different docking programs Flo+ [30], Surflex [31], and FRED [32] and six different data sets. We docked each database of actives and decoys to six pharmaceutically relevant targets retaining multiple poses. First, we calculated the enrichment rates using only the top-scoring pose of each compound for each target. Subsequently we passed all the poses of each compound through the pharmacophores generated from the co-crystallized complexes. After this process the enrichment rates were re-calculated based on the best scoring passing pose of each compound and compared to the enrichment rates obtained from docking alone (Fig. 1).

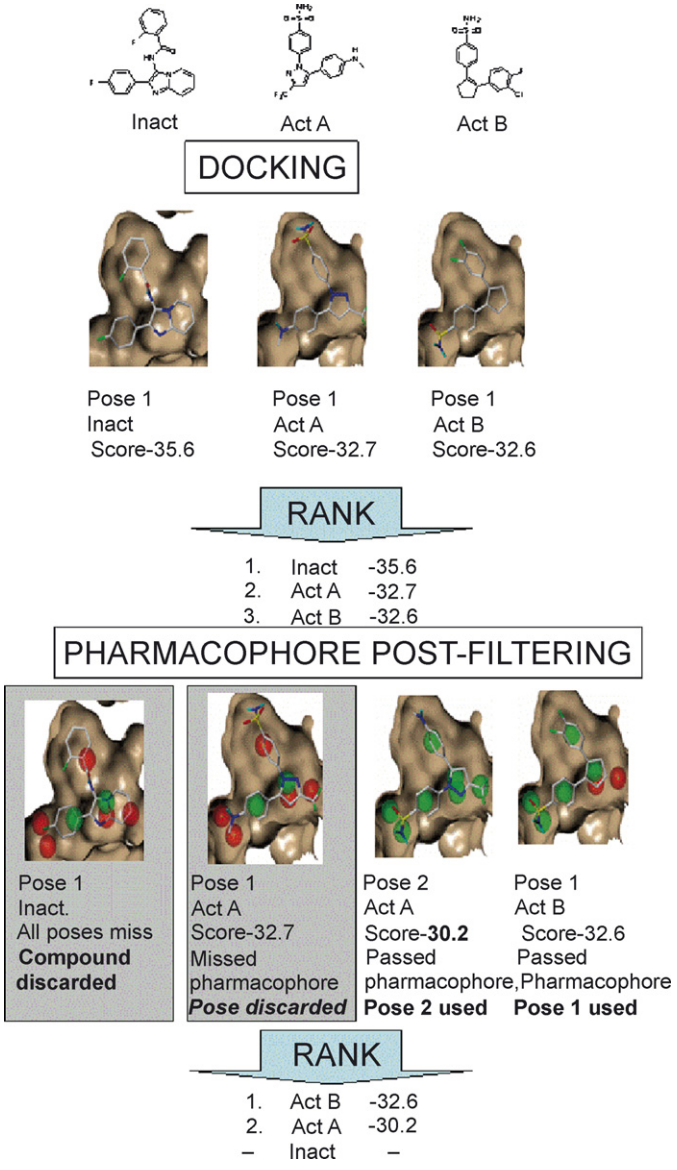


Fig. 1. Schematic representation of the approach using one decoy compound (Inact.) and two COX2 inhibitors (Act A and Act B). Compounds are first ranked according to scores alone and enrichment rates are calculated. All generated poses for all compounds are then passed through a pharmacophore filter. Those poses that do not fit the filter are discarded. The database is re-ranked and a new enrichment factor is calculated based on the best scored pose of each compound. A matched feature is colored green and a missed pharmacophore feature is colored red. Non-polar hydrogens are omitted for clarity.

## 2. Methods

### 2.1. Selection and preparation of protein complexes

The six reference protein complexes [33–38] used for docking were taken from the Brookhaven Protein DataBank [39] and are listed in Table 1. They were chosen to represent a variety of protein classes, differing in chemical characteristics and binding site shapes, encompassing both small-enclosed pockets such as ER$\alpha$ and large open pockets as in fXa. The selection of a particular crystal structure for docking among the available co-crystals was done by considering the resolution of the complex and the size of the co-crystallized ligand. Bound ligands, cofactors and metal ions were then removed except for the $Zn^{2+}$ ion present in MMP3 (1CIZ), which has been implicated in ligand binding [37]. As the coordinates of the bound water molecules depend on the types of ligands in the active sites, all water molecules were removed from the protein complexes. Addition of hydrogen atoms and the definition of the protein active site were determined by the requirements of the respective programs and will be discussed later.

### 2.2. Dataset generation

The datasets used in this study has previously been compiled previously compiled by Jacobsson and Karlén [40], and consists of known actives (available in Supporting Information) taken from the literature [41–48] against each of the six proteins pooled with 10,000 decoy molecules. These decoys were selected from a database of commercially available compounds after having passed Lipinskís rule of 5 filter (allowing 1

Table 1
Characteristics of the investigated targets and known actives

| PDB code[a] | Protein | Target type | No. of co-crystals ligands used[b] | Total no. of active compounds | Total no. of structures[c] |
|---|---|---|---|---|---|
| 1H00 [33] | CDK2 | Kinase | 44 | 98 | 249 |
| 6COX [34] | COX2 | Cyclo-oxygenase | 5 | 310[d] | 486 |
| 1L2I [35] | ERα | Nuclear hormone receptor | 5 | 151 | 618 |
| 1IQE [36] | fXa | Serine protease | 26 | 155 | 242 |
| 1CIZ [37] | MMP3 | Metallo-protease | 14 | 110 | 696 |
| 1F8D [38] | NA | Viral coat glycoprotein | 10 | 50[e] | 296 |

[a] PDB code of protein used in docking. The ligand of these co-complexes were used as templates for generating the different pharmacophores.
[b] Co-crystallized ligands available at the time was used to augment the set of known actives.
[c] Structure corresponds to all different enantiomers, tautomers and protonation states of a compound.
[d] Ligand structures kindly provided by Robert D. Clark.
[e] The stereoizer part of LigPrep is not used, since some actives are enantiomers of each other.

exception) [49]. The decoys along with the actives were further subjected to LigPrep [50] to generate all possible enantiomeric, tautomeric and protonation states. We assume that all chiral compounds in the dataset are present as racemates when purchased, and in subsequent analysis we are therefore not distinguishing between enantiomers. This means that there is a chance that a potentially inactive enantiomer of a confirmed active compound is falsely identified as active by the screen and treated as active throughout the analysis. This expanded set of compounds was energy minimized with the OPLS-AA force-field [51] resulting in a final database of 18,851 decoys (structures) corresponding to 9997 unique compounds with varying numbers of the actives yielding six different databases (Table 1). The reason for the decrease in the size of the database was that three compounds were filtered off during minimization, since they could not be handled correctly by the OPLS-AA force field. The minimized structures were converted into sd format (MDL Information Systems) using the *sdconvert* utility from Schrödinger. The resulting sd files were then converted into suitable formats for each software. Flo's internal sdconverter was used to produce the ligands in compressed MacroModel format for use in zdock+. Surflex was run with the ligands in mol2 format generated in SYBYL v.7.0 [52]. The sd files were submitted to OMEGA v. 1.8.1 [53] to generate conformers for use in FRED.

### 2.3. General docking

Since the overall aim of the study was to investigate the effect of post-filtering and not to compare different docking programmes, the docking protocols were setup using the programs default settings. No target specific optimizations were performed to increase the enrichment rates from docking or filtering, and the poses were scored with one of the program's internal scoring function. The six databases of structures were docked, with three different docking programs, retaining 10 poses of each of the 18851 decoy structures and varying number of active structures, rendering 18 docked databases. Only the highest scoring structure of each compound was considered for the first enrichment rate calculation. The three docking programs have very different pose generation algorithms and therefore the results presented in this study should be of general nature, and probably also valid for other docking softwares.

#### 2.3.1. Zdock+ v.0403

For databases and large combinatorial library screens zdock+ is the recommended Flo+ utility, which does a fast near systematic docking employing a Monte Carlo method for generating conformations and uses a modified version of the AMBER force field. We employed the *autocol* utility of Flo+ to generate guide atoms, which direct the grid map representation of the binding site. In some cases minor modifications were made to the recommended guide atoms based on visual inspection of the suggested binding pocket. Zdock+ has the possibility of introducing flexibility in the active site and include zero-order bonds to guide docking, but in this study all residues were kept fixed and no constraints were used.

A workset of 14 or 15 Å was cut around the co-crystallized ligand and the ligand was removed. In accordance with the recommendations of the authors, only polar hydrogens were added to the proteins and ligands. Lysines, arginines, aspartic and glutamic acids were kept positively and negatively charged, respectively. Default settings were used for all runs and the internal scoring, FreE, which estimates the free energy of the complex was used for ranking the docked complexes.

#### 2.3.2. Surflex v.1.27

Surflex is a docking method that combines Hammerhead's empirical scoring function [54] with morphological similarity to generate putative poses of ligand fragments and is mainly developed as a virtual screening tool. It uses an idealized active site ligand named protomol as a target to generate these poses. Here the protomol was generated using the co-crystallized complexes (Table 1) and no manual alterations were made. Polar as well as non-polar hydrogens were added to the proteins, which were kept in their appropriate ionization state at pH 7, i.e. protonated lysines and arginines while deprotonated glutamic and aspartic acids. The Surflex dockings were run using default settings employing the *whole molecule* approach. As recommended, the results from the Surflex runs were post-processed to penalize compounds that showed a pen score lower than 0.0 to filter out poses that penetrate the protein wall. It has been showed that in some cases other pen-values give

better enrichments, but in this work we have not explored this possibility to fine-tune the scoring [31].

#### 2.3.3. OMEGA v.1.8.1 and FRED v.2.1.1

The third docking approach used in this study is the combined OMEGA and FRED approach from OpenEye Scientific Software. It consists of a conformer generator, OMEGA, coupled with a fast rigid docking (FRED) of the pre-generated conformations. In FRED it is possible to utilize constrained docking, but this option was not used. OMEGA was run using an SD file as input, keeping conformations within 5.0 kcal/mol (e_window), having an rmsd cutoff of 0.6 Å (rms) and keeping 1000 output conformations in accordance with recomendation by Boström et al. [55].

The generated poses were ranked using the implemented Screenscore function [56]. Several other scoring functions are also available together with a consensus score in FRED, for consistency we chose to always use Screenscore even though it may not the best choice in all cases. The protein was prepared in the same way as for Surflex and the active site box was extended 4.0 Å around the co-crystallized ligand.

### 2.4. Pharmacophore generation and pharmacophore post-filtering

Peter Gund coined a widely used definition of a pharmacophore as a set of structural features responsible for a molecules biological activity [57]. Since in this work we only use information of one compound we are not able to derive a ''true'' pharmacophore. We instead try to identify potential pharmacophoric features within a given co-complexed ligand and will use the term pharmacophore to refer to the used set of such potential pharmacophoric features.

The pharmacophore filters were generated in an automated fashion from the ligand in the co-crystallized complex used for docking. The ''Model query from alignment'' option in UNITY [58] was used to suggest pharmacophoric points. Only suggested points residing on the ligand were kept in the final filters. The different features were divided into two groups, one that contained hydrophobic features and the remaining features were collected in a ''hetero'' group (Donor atom, Acceptor atom, Negative centers, and Positive nitrogens). The number of features in each group and for each target is shown in Table 2. To investigate how different pharmacophore settings, i.e. size tolerance of a feature and number of features to match, influence performance we explored them in a systematic fashion. We generated four pharmacophore filters with different complexities for each target, except NA, in which only two filters was used. Firstly, the influence of the tolerance criteria was probed by employing two different settings, a tight 1.0 Å (denoted $T^{1A}$) setting and a loose 2.0 Å (denoted $T^{2A}$) setting. Secondly, we also probed the effect of requiring different fractions of features to be matched by using two alterative settings. A stringent setting (denoted $F^{St}$) demanding fulfillment of at least 33% of all suggested ''hetero'' features and 50% of all hydrophobic features. The other more allowing setting (denoted $F^{Al}$) required the fulfillment of at least 20% of the ''hetero'' features and 25% of the hydrophobic features. The settings were combined in a systematic fashion and the four resulting pharmacophore filters are referred to as $T^{1A}$-$F^{St}$, $T^{1A}$-$F^{Al}$, $T^{2A}$-$F^{St}$, and $T^{2A}$-$F^{Al}$.

All docked poses from the different docking programs were passed through the four filters employing a 3D search in UNITY with no translation or rotation, and only those poses that passed the different pharmacophore filters were considered in the subsequent analysis. Lipinski filtering was turned off in this search. The best scoring passing pose of each compound was kept and enrichments factors together with receiver operator characteristics (ROC) [59] curves were recalculated.

To test the filters ability to return actives, the active compounds were subjected to a flexible search within UNITY, with no consideration of the active site. The most demanding ($T^{1A}$-$F^{St}$) and the most allowing ($T^{2A}$-$F^{Al}$) filters were employed in this test (Table 2). Default settings were used, with the exception of the Lipinski filter, which was turned off, and those compounds that were timed-out were given more time in a subsequent search(es) until they were discarded or approved.

## 3. Results and discussion

### 3.1. Dataset description

To establish that the decoys are representative of the six data sets we calculated a set of physico-chemical properties and studied the distribution of these (Fig. 2). From the plot showing molecular weight, it can be seen that the ERα inhibitors are relatively small while the MMP3 inhibitors showed a trend towards having high molecular weights. The decoys have a molecular weight distribution similar to the other data sets. The

Table 2
Number of features identified in the automatic pharmacophore generation (Hydrophobic (Hy.), Hetero (Het.)), and the minimum features to fulfil for the different filters, together with the percent of active compounds passing the most stringent and most allowing filter

| Target | #Hy. | ($F^{Al}$, $F^{St}$) | #Het. | ($F^{Al}$, $F^{St}$) | % fulfilling filter $T^{1A}$-$F^{St}$ | % fulfilling filter $T^{2A}$-$F^{Al}$ |
|---|---|---|---|---|---|---|
| CDK2 | 3 | (1, 2) | 11 | (3, 4) | 59 | 100 |
| COX2 | 4 | (1, 2) | 3 | (1, 1) | 100 | 100 |
| ERα | 4 | (1, 2) | 4 | (1, 2) | 93 | 99 |
| fXa | 4 | (1, 2) | 10 | (2, 4) | 17 | 100 |
| MMP3 | 5 | (2, 3) | 9 | (2, 3) | 92 | 100 |
| NA | 0 | (0, 0) | 14 | (3, 5) | 98 | 100[a] |

[a] For NA $T^{1A}$-$F^{Al}$ was the most allowing filter used.

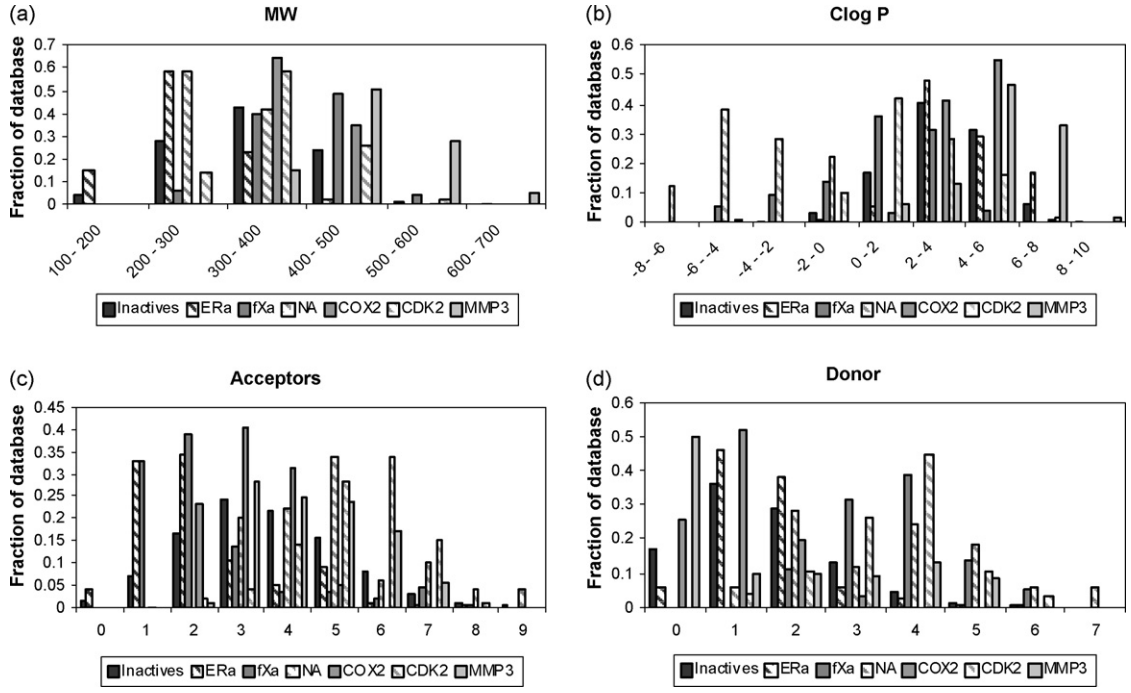


Fig. 2. The distribution of various physico-chemical descriptors computed for the compound database. (a) Molecular weight (MW), (b) CLOGP (c) Number of hydrogen bond acceptors, (d) Number of hydrogen bond donors. Note: 19 inactives together with 1 CDK2 active are not shown in graph (c) since they contain more than 9 acceptors. One inactive compound together with one CDK2 and one ERα inhibitor, are not shown in graph d since they contain more than 7 donors.

graph of CLOGP values showed that the NA data set was the most polar whereas the MMP3 data set was the most lipophilic with a CLOGP value as high as 8.0. This shows that the investigated compounds have a large spread in lipophilicity. The high polarity of the NA compounds is also reflected by the presence of a relatively large number of hydrogen bond donors and acceptors.

A principal component analysis (PCA) was used to project the compounds in principal component space to compare the decoys with the actives, using SIMCA-P+ v.11.0 [60]. A two component model was derived that explained 71% of the variance ($R^2X = 0.705$). The first component mainly describes size, while the second component describes lipophilicity. Small polar compounds, like the NA inhibitors end up in the upper left corner and large lipophilic compounds like the MMP3 inhibitors are positioned in the lower right corner. Taken together this not only showed that the decoy compounds covered the space of the actives but also that the actives of the different targets are structurally diverse (Fig. 3).

### 3.2. Virtual screening

The success of a virtual screening campaign can be assessed with several different metrics. In this study we choose to use the enrichment factor (EF) which is the relative enrichment of true positives in the fraction of the data set predicted to be active, where a random selection of compounds would yield an EF of 1. It was calculated using Eq. (1),

$$\mathrm{EF} = \frac{\mathrm{tp}/(\mathrm{tp}+\mathrm{fp})}{A/T} \quad (1)$$

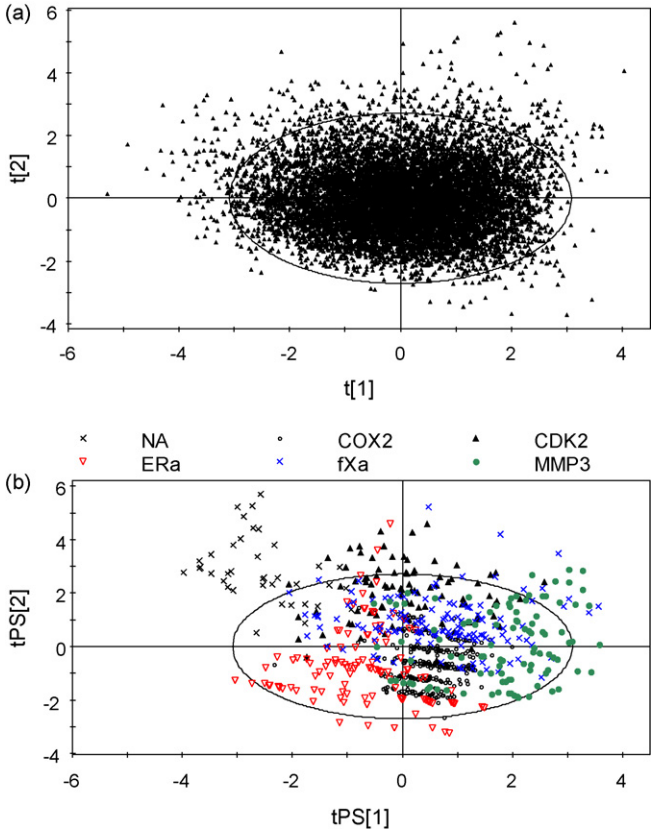


Fig. 3. Comparison of how the different classes of actives are distributed in the principal property space: (a) a two component score plot from PCA showing the spread of decoys; (b) predicted score values of the active compounds. In Fig. 2(b) one CDK2 and one ERα ligand have been excluded for clarity.

Table 3
Enrichment rates calculated at different sizes of the original database for docking alone and after pharmacophore filtering against CDK2

| | 1% | 3% | 5% | 10% |
|---|---|---|---|---|
| Zdock+ docking | 21.4 | 10.9 | 8.5 | 5.7 |
| $T^{1A}$-$F^{St}$ | 1/5[a] | – | – | – |
| $T^{1A}$-$F^{Al}$ | 6.1 | – | – | – |
| $T^{2A}$-$F^{St}$ | **30.8** | **15.0** | **10.3** | 5.7 |
| $T^{2A}$-$F^{Al}$ | **25.0** | **13.4** | **10.3** | **6.4** |
| Surflex docking | 27.3 | 16.3 | 11.6 | 6.8 |
| $T^{1A}$-$F^{St}$ | 1/8[a] | – | – | – |
| $T^{1A}$-$F^{Al}$ | 2.0 | – | – | – |
| $T^{2A}$-$F^{St}$ | **34.3** | 14.6 | 9.6 | 5.1 |
| $T^{2A}$-$F^{Al}$ | **40.6** | **20.7** | **13.7** | **7.4** |
| FRED docking | 8.2 | 4.1 | 4.1 | 3.9 |
| $T^{1A}$-$F^{St}$ | 15/43[a] | – | – | – |
| $T^{1A}$-$F^{Al}$ | **37.7** | **21.1** | **13.5** | – |
| $T^{2A}$-$F^{St}$ | **25.5** | **16.3** | **12.8** | **7.8** |
| $T^{2A}$-$F^{Al}$ | **9.2** | **8.5** | **7.5** | **4.9** |

Boldfaced numbers indicates an improvement compared to docking alone, and underscored values represent the highest enrichment within each program and database size.

[a] Very few compounds passed the filter. Results are reported as number of actives over total number of compounds passing the filter (active/total).

Table 5
Enrichment rates calculated at different sizes of the original database for docking alone and after pharmacophore filtering against ERα

| | 1% | 3% | 5% | 10% |
|---|---|---|---|---|
| Zdock+ docking | 33.9 | 14.5 | 10.1 | 6.1 |
| $T^{1A}$-$F^{St}$ | **47.4** | **18.2** | **11.1** | – |
| $T^{1A}$-$F^{Al}$ | **43.9** | **20.3** | **13.0** | **7.3** |
| $T^{2A}$-$F^{St}$ | **42.4** | **20.9** | **13.9** | **8.2** |
| $T^{2A}$-$F^{Al}$ | **37.2** | **17.9** | **12.0** | **6.9** |
| Surflex docking | 23.1 | 12.1 | 8.1 | 4.7 |
| $T^{1A}$-$F^{St}$ | **46.8** | – | – | – |
| $T^{1A}$-$F^{Al}$ | **37.3** | **17.6** | **12.3** | **7.5** |
| $T^{2A}$-$F^{St}$ | **36.6** | **16.9** | **12.8** | **7.7** |
| $T^{2A}$-$F^{Al}$ | **31.3** | **13.8** | **9.5** | **5.8** |
| FRED docking | 8.0 | 9.0 | 7.4 | 4.3 |
| $T^{1A}$-$F^{St}$ | **46.6** | – | – | – |
| $T^{1A}$-$F^{Al}$ | **33.9** | **15.6** | **11.1** | **7.0** |
| $T^{2A}$-$F^{St}$ | **35.3** | **12.8** | **12.6** | **8.0** |
| $T^{2A}$-$F^{Al}$ | **21.3** | **12.8** | **8.3** | **5.6** |

Boldfaced numbers indicates an improvement compared to docking alone, and underscored values represent the highest enrichment within each program and database size.

where tp is the number of true positives, defined as active compounds selected by the algorithms. Similarly fp represents the decoys falsely predicted to be active. *A* is the total number of known actives in each target database and *T* is the total number of compounds (actives and inactives) screened for each target. Tables 3–8 shows the enrichment factors for the top 1%, 3%, 5% and 10% of the total database for each of the six targets for all docking programs and all pharmacophore filters. The pharmacophore filtering often leads to considerable database reduction and we always consider a compound with no passing poses as being classified as inactive. Thus the EF after filtration cannot always be calculated at the higher percentages of the original database.

To graphically show the cumulative enrichment of actives we present the ROC curves [59] for the dockings in Figs. 4–9. These are based upon the two measurements selectivity

Table 4
Enrichment rates calculated at different sizes of the original database for docking alone and after pharmacophore filtering against COX2

| | 1% | 3% | 5% | 10% |
|---|---|---|---|---|
| Zdock+ docking | 22.0 | 18.1 | 13.8 | 8.6 |
| $T^{1A}$-$F^{St}$ | **32.3** | **29.7** | **19.3** | **9.8** |
| $T^{1A}$-$F^{Al}$ | **32.0** | **27.9** | **19.1** | **9.7** |
| $T^{2A}$-$F^{St}$ | **28.1** | **22.0** | **16.3** | **9.2** |
| $T^{2A}$-$F^{Al}$ | **27.5** | **21.7** | **15.8** | **9.1** |
| Surflex docking | 19.7 | 18.2 | 14.5 | 8.9 |
| $T^{1A}$-$F^{St}$ | **32.0** | **28.5** | **18.3** | **9.7**[a] |
| $T^{1A}$-$F^{Al}$ | **29.7** | **25.5** | **17.9** | **9.1** |
| $T^{2A}$-$F^{St}$ | **25.5** | **22.7** | **17.1** | **9.3** |
| $T^{2A}$-$F^{Al}$ | **24.0** | **21.7** | **16.5** | **9.1** |
| FRED docking | 31.6 | 18.8 | 12.9 | 7.4 |
| $T^{1A}$-$F^{St}$ | **32.9** | **23.7** | **15.1** | **8.2** |
| $T^{1A}$-$F^{Al}$ | **32.9** | **22.6** | **14.6** | **7.7** |
| $T^{2A}$-$F^{St}$ | **32.6** | **20.8** | **14.5** | **7.7** |
| $T^{2A}$-$F^{Al}$ | **32.6** | **20.7** | **14.3** | **7.7** |

Boldfaced numbers indicates an improvement compared to docking alone, and underscored values represent the highest enrichment within each program and database size.

[a] Only 9.5% of the original database remained after filtering.

Table 6
Enrichment rates calculated at different sizes of the original database for docking alone and after pharmacophore filtering against fXa

| | 1% | 3% | 5% | 10% |
|---|---|---|---|---|
| Zdock+ docking | 8.9 | 5.6 | 4.3 | 3.6 |
| $T^{1A}$-$F^{St}$ | 0/1[a] | – | – | – |
| $T^{1A}$-$F^{Al}$ | **9.6** | **5.7** | 4.1 | 2.1 |
| $T^{2A}$-$F^{St}$ | 2.6 | 1.7 | 1.4 | – |
| $T^{2A}$-$F^{Al}$ | 8.1 | 5.5 | **5.0** | **3.7** |
| Surflex docking | 19.1 | 10.9 | 9.1 | 6.6 |
| $T^{1A}$-$F^{St}$ | 0/0[a] | – | – | – |
| $T^{1A}$-$F^{Al}$ | 18.0 | 10.2 | 7.1 | – |
| $T^{2A}$-$F^{St}$ | **20.5** | 8.6 | 5.7 | – |
| $T^{2A}$-$F^{Al}$ | **21.2** | **14.3** | **11.2** | **7.7** |
| FRED docking | 8.9 | 8.2 | 8.1 | 7.0 |
| $T^{1A}$-$F^{St}$ | 4/4 | – | – | – |
| $T^{1A}$-$F^{Al}$ | **19.9** | **12.9** | **8.6** | 4.4 |
| $T^{2A}$-$F^{St}$ | **10.9** | 7.7 | 6.1 | 3.4 |
| $T^{2A}$-$F^{Al}$ | **10.9** | **9.9** | 8.1 | **6.7** |

Boldfaced numbers indicates an improvement compared to docking alone, and underscored values represent the highest enrichment within each program and database size.

[a] Very few compounds passed the filter. Results are reported as number of actives over total number of compounds passing the filter (active/total).

Table 7
Enrichment rates calculated at different sizes of the original database for docking alone and after pharmacophore filtering against MMP3

| | 1% | 3% | 5% | 10% |
|---|---|---|---|---|
| Zdock+ docking | 2.6 | 3.5 | 3.6 | 3.6 |
| $T^{1A}$-$F^{St}$ | 2/3[a] | – | – | – |
| $T^{1A}$-$F^{Al}$ | **17.7** | – | – | – |
| $T^{2A}$-$F^{St}$ | **12.5** | **9.4** | **7.3** | **5.8** |
| $T^{2A}$-$F^{Al}$ | **3.5** | **6.7** | **6.7** | **4.5** |
| Surflex docking | 41.8 | 23.7 | 15.5 | 8.1 |
| $T^{1A}$-$F^{St}$ | 1/5[a] | – | – | – |
| $T^{1A}$-$F^{Al}$ | **48.2** | – | – | – |
| $T^{2A}$-$F^{St}$ | **44.6** | 18.7 | 12.2 | – |
| $T^{2A}$-$F^{Al}$ | **43.7** | **24.3** | **15.6** | **8.8** |
| FRED docking | 25.5 | 13.0 | 10.0 | 5.6 |
| $T^{1A}$-$F^{St}$ | 5/13[a] | – | – | – |
| $T^{1A}$-$F^{Al}$ | **27.3** | 12.7 | 8.6 | – |
| $T^{2A}$-$F^{St}$ | **29.1** | 12.4 | 8.2 | 4.5 |
| $T^{2A}$-$F^{Al}$ | **29.1** | **15.5** | **10.4** | 5.5 |

Boldfaced numbers indicates an improvement compared to docking alone, and underscored values represent the highest enrichment within each program and database size.
[a] Very few compounds passed the filter. Results are reported as number of actives over total number of compounds passing the filter (active/total).

(Se) and specificity (Sp) presented in Eqs. (2) and (3), respectively.

$$\mathrm{Se} = \frac{\mathrm{tp}}{A} \tag{2}$$

$$\mathrm{Sp} = \frac{\mathrm{tn}}{I} \tag{3}$$

In Eq. (3) tn is the number of true negatives, i.e. inactive compounds classified as inactives, and $I$ is the total number of inactives in the database. Since ROC curves plot the sensitivity (ability to pick actives) as a function of specificity (ability to discard inactives) they contain an extra dimension of information that is not present in cumulative enrichment graphs, which are only concerned with sensitivity.

Table 8
Enrichment rates calculated at different sizes of the original database for docking alone and after pharmacophore filtering against NA

| | 1% | 3% | 5% | 10% |
|---|---|---|---|---|
| Zdock+ docking | 8.0 | 9.1 | 8.7 | 7.2 |
| $T^{1A}$-$F^{St}$ | **76.4** | – | – | – |
| $T^{1A}$-$F^{Al}$ | **34.8** | **24.2** | **16.0** | **9.4** |
| Surflex docking | 48.2 | 23.9 | 15.8 | 9.0 |
| $T^{1A}$-$F^{St}$ | **72.3** | – | – | – |
| $T^{1A}$-$F^{Al}$ | **56.3** | **26.5** | **17.2** | **9.8** |
| FRED docking | 0 | 0 | 0 | 0.2 |
| $T^{1A}$-$F^{St}$ | **36/61**[a] | – | – | – |
| $T^{1A}$-$F^{Al}$ | **4.0** | **9.3** | **10.3** | **9.5**[b] |

Boldfaced numbers indicates an improvement compared to docking alone, and underscored values represent the highest enrichment within each program and database size.
[a] Very few compounds passed the filter. Results are reported as number of actives over total number of compounds passing the filter (active/total).
[b] at 9.7% of the screened database.

### 3.2.1. Cyclin dependent kinase 2 (CDK2)

The binding site of CDK2 is a hydrophobic slot, positioned in between the two domains of the kinase. It is a flexible site that can accommodate diverse ligands, as reflected in the PCA score plot in Fig. 3 where the CDK2 inhibitors span a large area. Important interactions are the hydrogen bonds between the ligand and the backbone of Leu83. Based on the scoring in zdock+ an enrichment of 5.7 at 10% was obtained (Table 3). Surflex gave a higher enrichment of 6.8 at 10%, also displaying good poses for the high scoring actives. FRED gave a low enrichment of 3.9 at 10%.

The large size of the co-crystallized ligand gave rise to a rather complex pharmacophore. Even though the known CDK2 inhibitors are structurally diverse (see Figs. 1 and 2, and Supporting Information) many compounds had the potential to fulfil the $T^{1A}$-$F^{St}$ setting (59%, Table 2). Still, when this filter was used as a post-filter after docking very few hits, and low enrichment rates were obtained (Table 3). This showed that although the compounds had the potential to fit the filter, the poses generated by the docking software inside the active site did not fit this pharmacophore. Increasing the size tolerance criteria had clear beneficial effects on enrichments in most cases. The number of features to be matched seemed to be of less importance, since both feature settings gave comparable results (Table 3). Slightly better performance was seen for the stringent setting, with more false positives being ruled out. Inspection of Fig. 4 indicates that the post-filtering process has the greatest impact in the case of FRED. It can also be seen that most pharmacophore filters discarded many false positives whereas many active compounds were retained, giving increased enrichments (Table 3 and Fig. 4c).

### 3.2.2. Cyclooxygenase 2 (COX2)

The binding pocket of COX2 is closed and mainly hydrophobic in nature. Within this hydrophobic cage is a charged amino acid, Arg120, which has been shown to be important for stabilizing the carboxylate moiety found in the classical NSAIDs [34]. The COX2 dataset used is comprised of 3 unselective COX inhibitors and 307 selective COX2 inhibitors. The docked top-scoring pose of the active compounds from all docking programs superimposed well when overlaid onto the co-crystallized structure of 6COX. These poses were also scored high, yielding enrichments above 7.4 at 10% of the database for all docking programs.

Since all docking programs produced good poses the observed increase in enrichment after pharmacophore filtering as compared to docking alone was expected (Fig. 5). It is also clearly seen that a more demanding pharmacophore is more efficient in this case, and it also seems that the size tolerance is more important than the matching of many features since the $T^{1A}$-$F^{Al}$ pharmacophore combination yields better enrichments than the $T^{2A}$-$F^{St}$ pharmacophore. This illustrates the fact that the docking programs in this case were able to produce high quality docking poses, close to the known co-crystal of 6COX, and that these poses were recognized by the pharmacophore filter. It is also seen in Table 4 that all docking programs in combination with the $T^{1A}$-$F^{St}$ filter have an EF that is close to

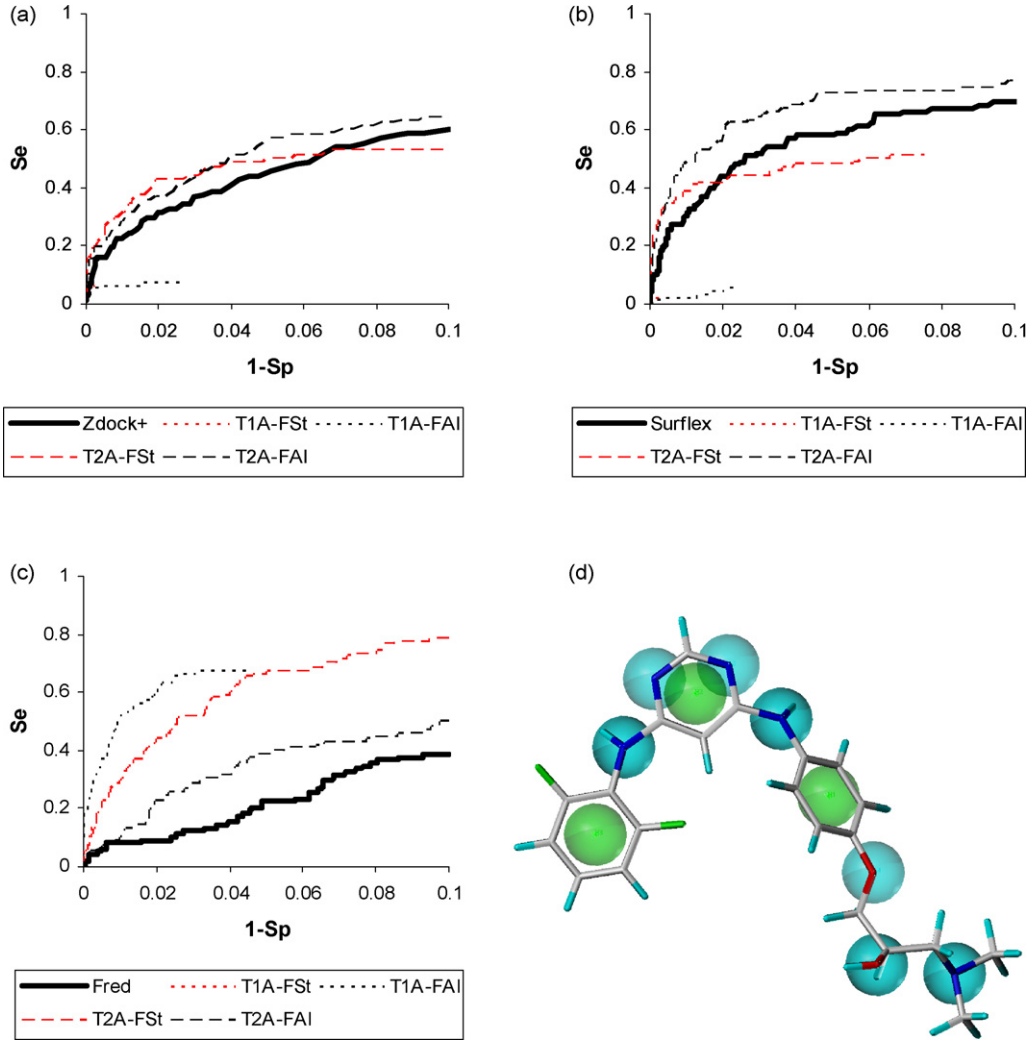


Fig. 4. CDK2 results: (a) ROC curve for zdock+ docking and after filtration; (b) ROC curve for Surflex docking and after filtration; (c) ROC curve for FRED docking and after filtration; (d) features (1 Å tolerance) identified in co-crystallized ligand of 1H00. 11 hetero features colored in cyan and 3 hydrophobic features shown in green.

the ideal value of 33.2 at 1% of the database. This indicates that the filtering works excellent in this case. It should however be noticed that the set of COX2 inhibitors are all rather similar as seen in Fig. 3 and Supporting Information, and all 310 compounds could pass the $T^{1A}$-$F^{St}$ pharmacophore in a flexible search in UNITY (Table 2).

### 3.2.3. Estrogen Receptor α (ERα)

The active site of the estrogen receptor α is closed and hydrophobic with two important hydrogen bonding regions, His524 on one side and Arg394 and Glu353 on the other side of the pocket. It is activated by small, hydrophobic molecules such as glucocorticoids and estrogens. Upon visual inspection it was seen that all docking programs placed the active ligands correctly, and between them zdock+ showed the best performance with an enrichment of 6.1 at 10%.

In all cases, pharmacophore post-filtering had a beneficial effect on enrichment as compared to docking alone. This effect is most pronounced for FRED, as shown by the enrichment factors at 1% of the screened database (Table 5) and in the ROC curve (Fig. 6c). Similarly to what was found for COX2, it was seen that the best results were often obtained when using the more stringent feature criteria and since most actives included in the study also fitted the most demanding pharmacophore ($T^{1A}$-$F^{St}$) in the flexible search (Table 2), this was not surprising. The very simple $T^{1A}$-$F^{Al}$ and $T^{2A}$-$F^{Al}$ pharmacophores only required 1 hydrophobic and 1 hetero feature to be found in the docked pose, which gave many passing poses and thereby reduced the filtering effect. A point worth mentioning is that nine active compounds from a different structural class, utilizing only half of the binding pocket, passed these allowing filters. This shows that it is possible to identify novel structural classes using this approach. Furthermore, the difference seen in enrichment between the three docking softwares before filtering is more or less removed after filtering.

### 3.2.4. Blood coagulation factor Xa (fXa)

The serine protease factor Xa is involved in a key step in the coagulation cascade. Inhibitors often encompass a basic P1

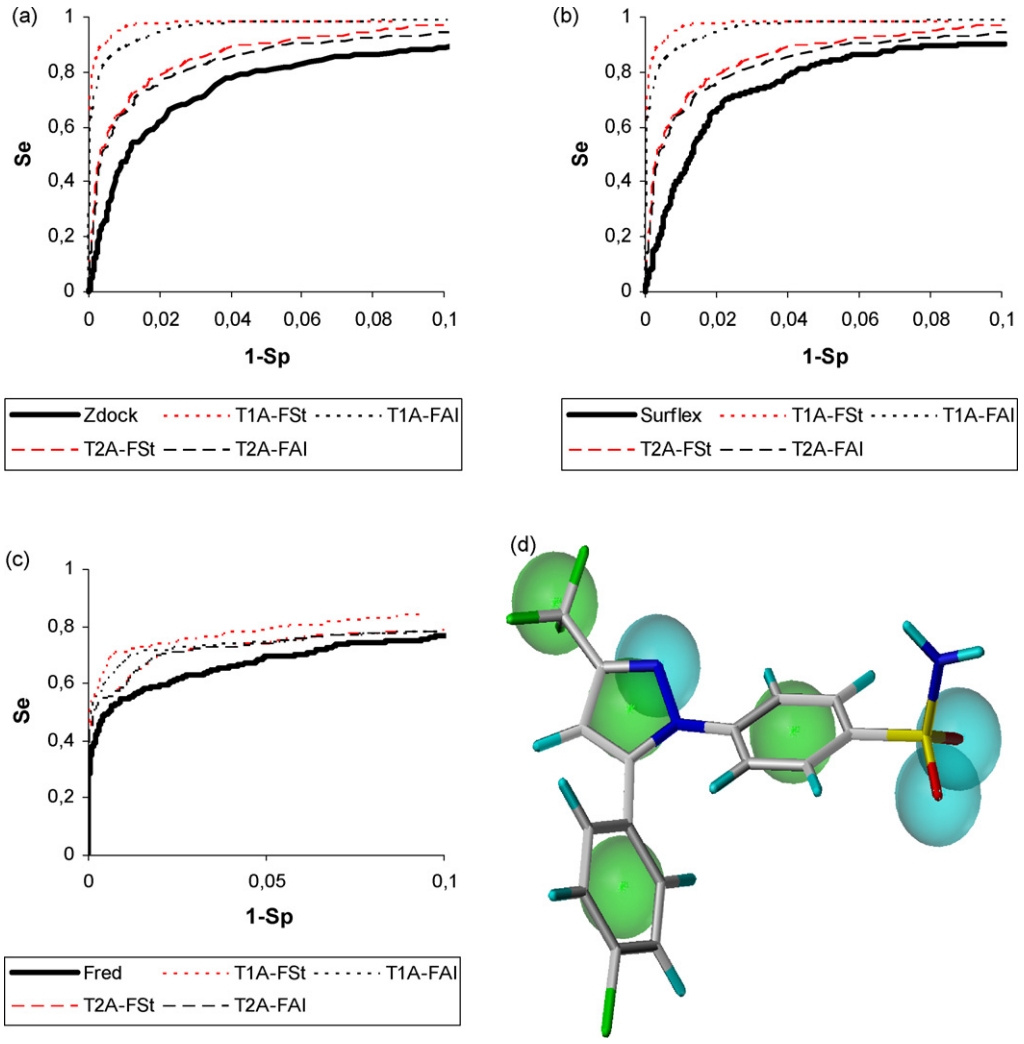


Fig. 5. COX2 results: (a) ROC curve for zdock+ docking and after filtration; (b) ROC curve for Surflex docking and after filtration; (c) ROC curve for FRED docking and after filtration; (d) features (1Å tolerance) identified in co-crystallized ligand of 6COX. 3 hetero features colored in cyan and 4 hydrophobic features shown in green.

group that mimic the native arginine residue binding in the S1 pocket forming an ionic interaction with Asp189. It has been shown that this interaction is not an absolute requirement for ligand binding and a new class of inhibitors has emerged containing arylhalides as P1 substituents, which enabled the development of more selective fXa inhibitors [61]. Here we include both classes of inhibitors, those having a basic P1 substituents and a smaller number with a P1 arylhalide substituent.

Zdock+ was able to place both the basic P1 substituent and P1 arylhalide correctly in the S1 pocket. In spite of this, the enrichment rate was only 3.6 at 10%, indicating that a large portion of false positives were also selected (Fig. 7). Also Surflex and FRED positioned the P1 group correctly, but scored the actives better, and therefore gave a higher enrichment of 6.6 and 7.0 at 10%, respectively.

A drop in the enrichment rates was found for all softwares after pharmacophore post-filtering using the stringent setting (Table 6), which was not surprising since only about 17% of the actives could pass the most demanding filter in the flexible search (Table 2). One reason for this is that the pharmacophore was built from a ligand incorporating a P1 arylhalide substituent, whereas the main part of the fXa active compounds was comprised of ligands with a basic P1 substituent. This highlight a potential pitfall associated with generating a pharmacophore based on only one compound, since that compound might not be representative of the actives. Still, when using the $F^{Al}$ setting an increase in enrichments could often be seen, especially in the early part of the databases, which shows that using a more allowing filter can help to solve this problem.

### 3.2.5. Matrix metalloprotease 3 (Stromelysin, MMP3)

MMP3 has been a commonly employed target in several docking evaluations and validations [7,46,62]. The presence of a $Zn^{2+}$ ion in the active site makes it an interesting test case. The inhibitors of MMP3 are often large and hydrophobic and contain a chelating moiety, which interacts with this zinc ion.

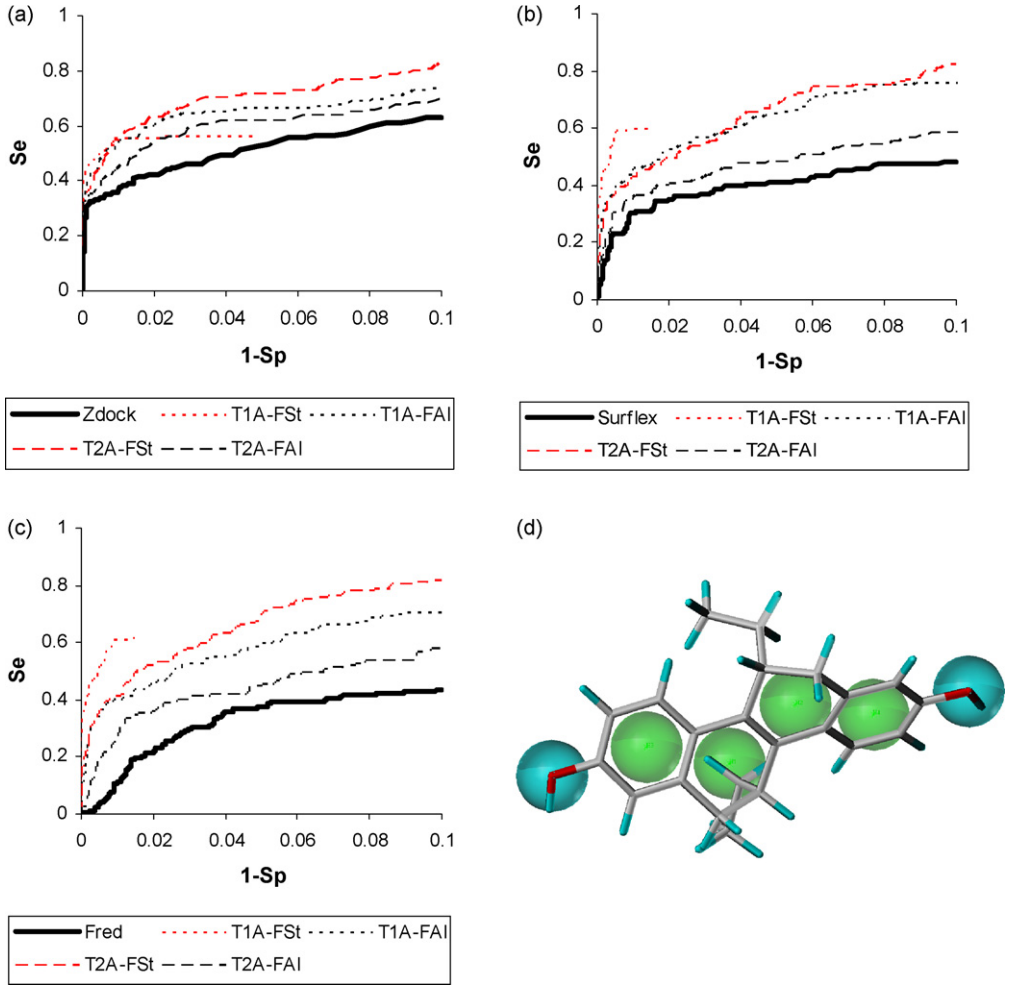


Fig. 6. ERα results: (a) ROC curve for zdock+ docking and after filtration; (b) ROC curve for Surflex docking and after filtration; (c) ROC curve for FRED docking and after filtration; (d) features (1Å tolerance) identified in co-crystallized ligand of 1L2I. 4 hetero features, 2 donor atoms and 2 acceptor atom, colored in cyan and 4 hydrophobic features shown in green. Note that the two hydroxyl groups give rise to both donor and acceptor features.

The MMP3 pocket poses a challenge in that it is open and hydrophobic in nature, which makes it difficult for the docking programs to position the hydrophobic side chains correctly in the active site while maintaining the interaction with the metal ion. A low enrichment of 3.6 at 10% with zdock+ suggested a poor scoring of the docked poses, which is also seen in Fig. 8. The increase in enrichment rates after pharmacophore filtering as compared to docking alone indicated that the inhibitors were correctly posed by zdock+ in spite of their poor scores. This was also verified by visual inspection. Surflex produced docking results of high quality and with a good discriminatory power in scoring. Some of the known active ligands are large with many rotatable bonds, and in the conformer generation with OMEGA, only 75 of 110 (68%) known actives could be processed with the settings used. This reduction of the total number of known actives in the final analysis made it more difficult to obtain high enrichment rates using FRED, since these are calculated according to the original number of actives (110).

The pharmacophore used in this case was rather complex, with many features. The benefits of post-filtering were not as clearly seen for the Surflex and FRED dockings as they were for zdock+, even though the enrichment rates were usually higher. Still, early on in the database all but the $T^{1A}$-$F^{St}$ pharmacophore gave an increased enrichment in all softwares (Table 7). Like in the case of fXa and CDK2 which also have complex pharmacophores, the $F^{Al}$ setting seemed to be best suited for filtering.

### 3.2.6. Neuraminidase (NA)

Neuraminidase has received attention as an anti-influenza target and Zanamavir, a neuraminidase inhibitor, was developed in one of the first successful structure-based drug design campaigns [63]. The active site of NA is highly conserved across different influenza strains and is mainly comprised of highly polar residues like arginine and glutamic acid. All of the actives included in our dataset are small and hydrophilic, containing a carboxylate moiety that is essential for electrostatic interactions with the three arginines Arg118, Arg292, and Arg371 in the active site [43]. In the scoring of the compounds Surflex was superior to zdock+ early in the database (Fig. 9). However, at 10% of the database both

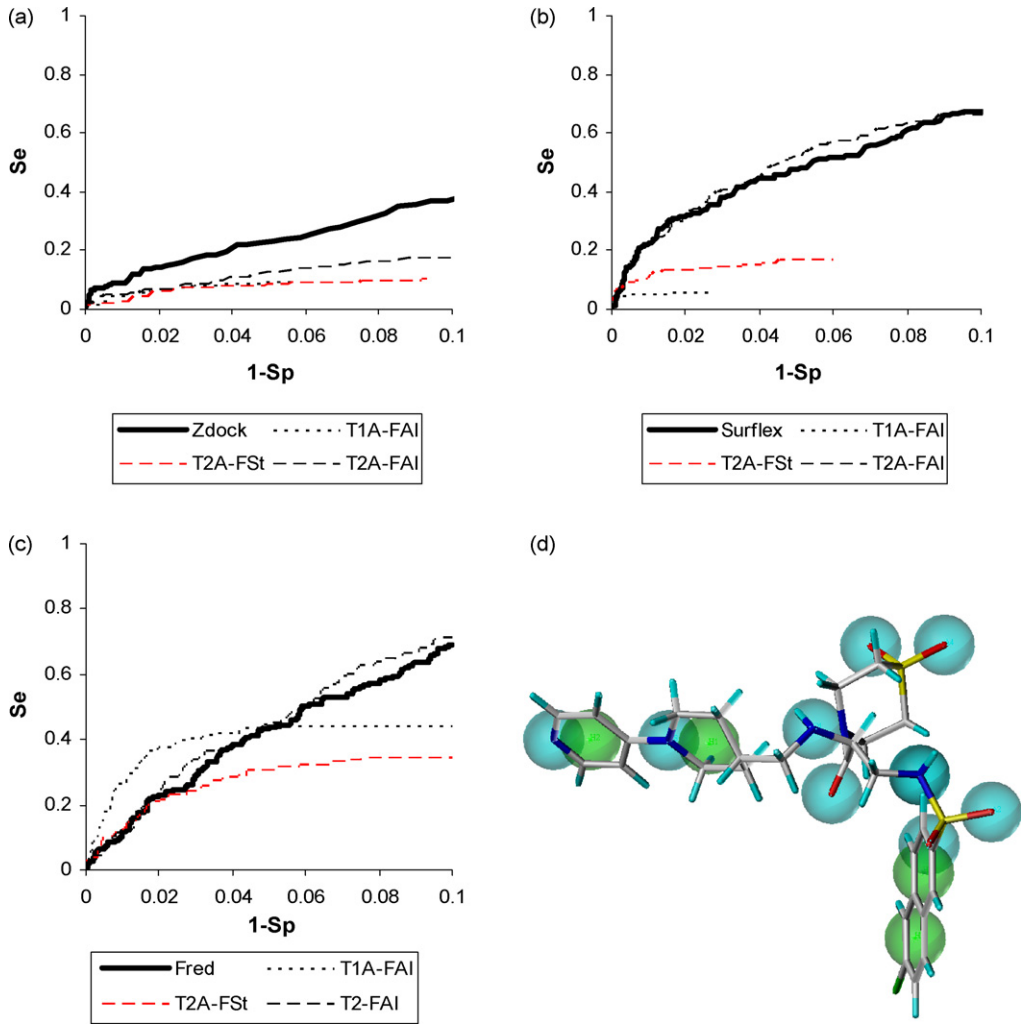


Fig. 7. fXa results: (a) ROC curve for zdock+ docking and after filtration; (b) ROC curve for Surflex docking and after filtration; (c) ROC curve for FRED docking and after filtration; (d) features (1 Å tolerance) identified in co-crystallized ligand of 1IQE. 10 hetero features colored in cyan and 4 hydrophobic features shown in green.

zdock+ and Surflex showed similar enrichment rates, whereas FRED had surprisingly low enrichment. Still, the posing algorithms of all programs often placed the carboxylate group in close proximity to the important arginines.

For the neuramidase target a rather complex pharmacophore was employed due to the many heteroatoms present in the small co-crystallized ligand. Despite this, almost all actives could fulfil the $T^{1A}F^{St}$ pharmacophore in the flexible search (Table 2). Furthermore, a rather large fraction of the docked databases could pass the $T^{1A}F^{Al}$ filter (depending on docking software approximately 1000–2000 compounds). In case of FRED (Fig. 9) many of the false positives were filtered away and the true positives were enriched after the pharmacophore filtration. This dramatic positive effect is clearly seen in Fig. 9c. For technical reasons we did not test all pharmacophore combinations in this case since UNITY was very slow at filtering, most likely due to the many overlapping features. Therefore only the $T^{1A}$-$F^{St}$ and $T^{1A}$-$F^{Al}$ settings were tested. Both these settings gave good enrichments, and the $T^{1A}$-$F^{St}$ setting showed almost ideal enrichments in all cases (Fig. 9). This indicates that if a complex pharmacophore is used in combination with a high quality pose generation, the results can be very good.

### 3.2.7. *Summary of the performance of different pharmacophore filters*

It was seen that most of the active compounds used in the study were able to fit the most demanding pharmacophore filter in a flexible search. However, in two cases, fXa and CDK2, many of the active compounds could not pass the $T^{1A}$-$F^{St}$ filter (Table 2). One reason for this was that the pharmacophores were built from only one compound, which was not representative of all active compounds. This is clearly seen for fXa, where many of the active compounds in the database are of a different chemical class as compared to the 1IQE ligand used for the filter creation. In the case of CDK2, the ligand used for generating the pharmacophore gave rise to many potential

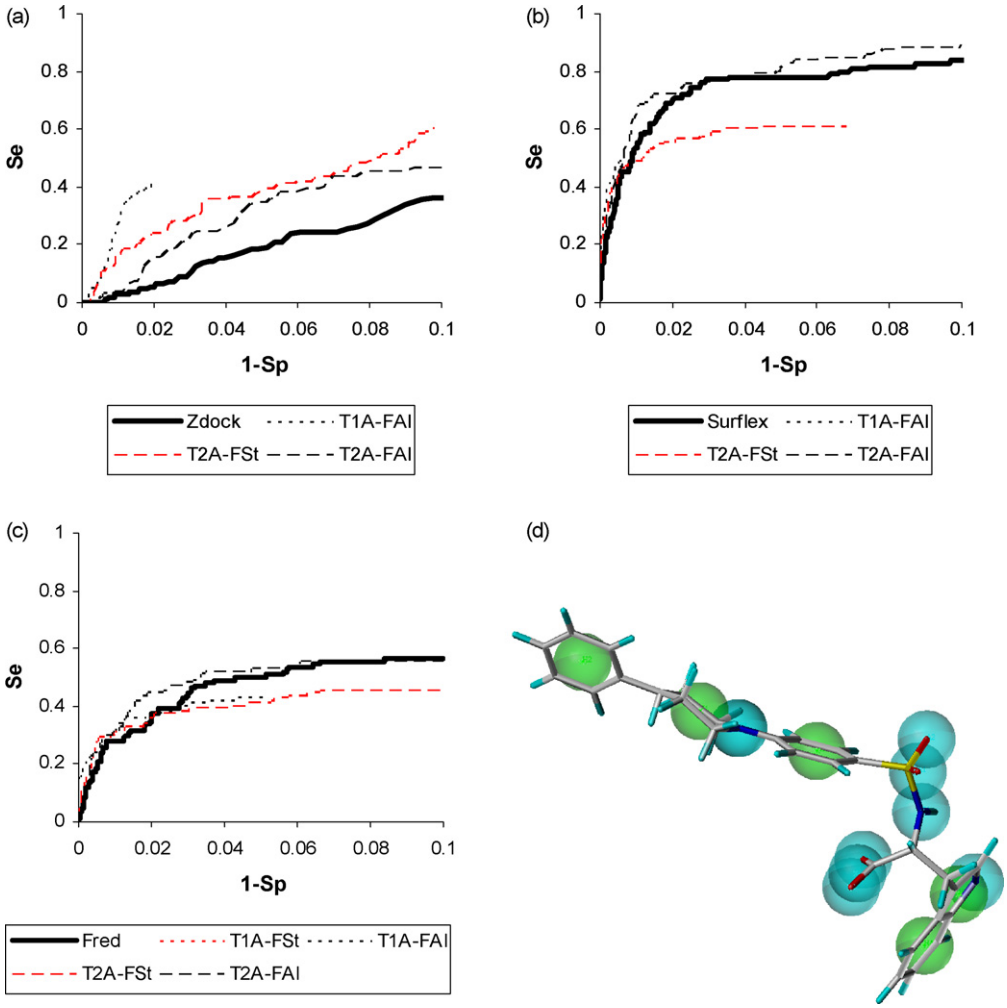


Fig. 8. MMP3 results: (a) ROC curve for zdock+ docking and after filtration; (b) ROC curve for Surflex docking and after filtration; (c) ROC curve for FRED docking and after filtration; (d) features (1 Å tolerance) identified in co-crystallized ligand of 1CIZ. 9 hetero features colored in cyan and 5 hydrophobic features shown in green. Note that secondary amine give rise to both an acceptor and a donor.

pharmacophore features, resulting in that this filter required the fulfillment of at least 6 features (2 hydrophobic and 4 hetero). These problems can be circumvented either by using a more allowing filter, or if available, by employing more ligand–target information. For example, Perola et al. utilized more target–ligand interaction and was thereby able to generate a simpler pharmacophore, which they used with great success in kinase virtual screens [21].

Table 9
Summary of the pharmacophore post-filter performance showing the number of times each filter gave better enrichments than docking alone at 1%, 3%, 5%, and 10% of the total database

| | 1% | 3% | 5% | 10% |
|---|---|---|---|---|
| $T^{1A}$-$F^{St}$ | **8** (**8**) | **4** (**4**) | **4** (**4**) | **3** (**3**) |
| $T^{1A}$-$F^{Al}$ | 15 (18) | 12 (14) | 11 (14) | 9 (11) |
| $T^{2A}$-$F^{St}$ | **14** (**15**) | 9 (15) | 9 (15) | 8 (12) |
| $T^{2A}$-$F^{Al}$ | **14** (**15**) | **14** (**15**) | **14** (**15**) | **14** (**15**) |

The number in parentheses shows the number of times the filter retains enough compounds to allow enrichment rate calculation. Boldface indicates that filtering improved enrichments in more than 90% of the cases for a given filter and cutoff.

It has been shown that post-filtering with pharmacophores often had a beneficial effect on enrichment rates and a summary of the performance of the different filters can be seen in Table 9. Given that there are enough compounds left after filtering to calculate enrichment rates at a certain cutoff, there is an improvement as compared to docking alone in 162 of 193 (84%) filter and cutoff combinations.

Some lessons concerning the construction and selection of the filters can also be learned. A more stringent filter often has a larger filtering effect, rendering very small databases, which usually are of high quality (Tables 3-8). By using the $T^{2A}$-$F^{Al}$ filter it was possible to calculate enrichments at 10% of the database for all targets, and results were improved compared to docking in 14 out of 15 trials. Importantly, the results from ERα and fXa also indicates that using an allowing filter setting might enable the identification of a different structural class of inhibitors as compared to the one used for creating the filter.

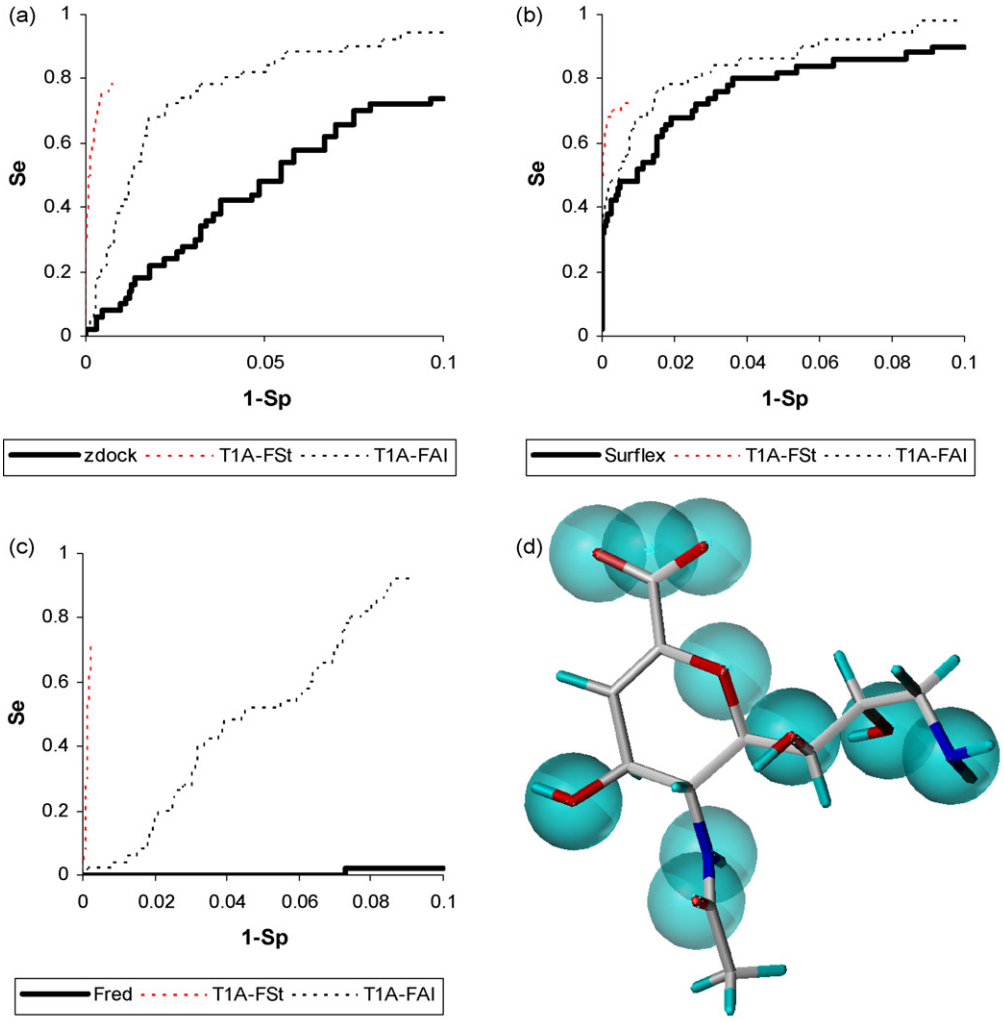


Fig. 9. NA results: (a) ROC curve for zdock+ docking and after filtration; (b) ROC curve for Surflex docking and after filtration; (c) ROC curve for FRED docking and after filtration; (d) features (1 Å tolerance) identified in co-crystallized ligand of 1F8D. 14 hetero features colored in cyan, note that hydroxyls and amine give rise to both donor and acceptor atoms.

## 4. Conclusion

We have investigated the performance of pharmacophores generated from X-ray complexes as a means of post-filtering docked compounds and their influence on enrichment. We hypothesized that this would aid in retaining only the more relevant poses and thereby increase enrichment rates. In this approach we save and analyze multiple poses of each compound, which may help us to overcome the docking problem. Results indicate that post-filtering with co-crystal-based pharmacophores most often has a beneficial effect on enrichment factors, since the number of false positives were decreased early in the database. The advantage of post-filtering is more pronounced when the scoring function performs poorly in ranking the poses but the posing algorithm works well, as seen for e.g. NA (zdock+, FRED). However, in a few setting combinations the enrichments calculated from docked scores were better than enrichment from pharmacophore post-filtered scores. It should be noted that this approach may not be successful when the pharmacophore filter is too complex, requiring many well localized features as seen for the $T^{1A}$-$F^{St}$ setting in CDK2, fXa, and MMP3. If the suggested pharmacophore contains many features a more allowing filter should be applied, otherwise the most stringent criteria should be used.

We have successfully highlighted the influence of pharmacophore mapping as a means of post-filtering. In conclusion: Docking alone gives enrichment over random screening, but when coupled with correctly defined pharmacophores it often leads to even higher enrichments.

## Acknowledgments

We express our sincere gratitude to the Swedish Foundation for Strategic Research (SSF) for financing this research.

## Appendix A. Supplementary data

Supplementary data associated with this article can be found, in the online version, at doi:10.1016/j.jmgm.2007.11.005.

## References


[1] J.A. DiMasi, R.W. Hansen, H.G. Grabowski, The price of innovation: new estimates of drug development costs, J. Health Econ. 22 (2003) 151–185.

[2] B.K. Shoichet, S.L. McGovern, B. Wei, J.J. Irwin, Lead discovery using molecular docking, Curr. Opin. Chem. Biol. 6 (2002) 439–446.

[3] T. Langer, R.D. Hoffmann, Virtual screening: an effective tool for lead structure discovery? Curr. Pharm. Des. 7 (2001) 509–527.

[4] E. Perola, W.P. Walters, P.S. Charifson, A detailed comparison of current docking and scoring methods on systems of pharmaceutical relevance, Proteins: Struct. Funct. Bioinform. 56 (2004) 235–249.

[5] C. Bissantz, G. Folkers, D. Rognan, Protein-based virtual screening of chemical databases. 1. Evaluation of different docking/scoring combinations, J. Med. Chem. 43 (2000) 4759–4767.

[6] E. Kellenberger, J. Rodrigo, P. Muller, D. Rognan, Comparative evaluation of eight docking tools for docking and virtual screening accuracy, Proteins: Struct. Funct. Bioinform. 57 (2004) 225–242.

[7] M. Kontoyianni, L.M. McClellan, G.S. Sokol, Evaluation of docking performance: comparative data on docking algorithms, J. Med. Chem. 47 (2004) 558–565.

[8] M.D. Eldridge, C.W. Murray, T.R. Auton, G.V. Paolini, R.P. Mee, Empirical scoring functions. I. The development of a fast empirical scoring function to estimate the binding affinity of ligands in receptor complexes, J. Comput. Aid. Mol. Des. 11 (1997) 425–445.

[9] M. Rarey, B. Kramer, T. Lengauer, G. Klebe, A fast flexible docking method using an incremental construction algorithm, J. Mol. Biol. 261 (1996) 470–489.

[10] M.L. Verdonk, J.C. Cole, M.J. Hartshorn, C.W. Murray, R.D. Taylor, Improved protein-ligand docking using GOLD, Proteins: Struct. Funct. Bioinform. 52 (2003) 609–623.

[11] T.J.A. Ewing, S. Makino, A.G. Skillman, I.D. Kuntz, Dock 4. 0: search strategies for automated molecular docking of flexible molecule databases, J. Comput. Aid. Mol. Des. 15 (2001) 411–428.

[12] P.S. Charifson, J.J. Corkery, M.A. Murcko, W.P. Walters, Consensus scoring: a method for obtaining improved hit rates from docking databases of three-dimensional structures into proteins, J. Med. Chem. 42 (1999) 5100–5109.

[13] R. Wang, L. Lai, S. Wang, Further development and validation of empirical scoring functions for structure-based binding affinity prediction, J. Comput. Aid. Mol. Des. 16 (2002) 11–26.

[14] R.D. Taylor, P.J. Jewsbury, J.W. Essex, A review of protein-small molecule docking methods, J. Comput. Aid. Mol. Des. 16 (2002) 151–166.

[15] D.B. Kitchen, H. Decornez, J.R. Furr, J. Bajorath, Docking and scoring in virtual screening for drug discovery: methods and applications, Nat. Rev. Drug Discov. 3 (2004) 935–949.

[16] G.L. Warren, C.W. Andrews, A.-M. Capelli, B. Clarke, J. LaLonde, M.H. Lambert, M. Lindvall, N. Nevins, S.F. Semus, S. Senger, G. Tedesco, I.D. Wall, J.M. Woolven, C.E. Peishoff, M.S. Head, A critical assessment of docking programs and scoring functions, J. Med. Chem. 49 (2006) 5912–5931.

[17] J. Tirado-Rives, W.L. Jorgensen, Contribution of conformer focusing to the uncertainty in predicting free energies for protein-ligand binding, J. Med. Chem. 49 (2006) 5880–5884.

[18] J.M. Jansen, E.J. Martin, Target-biased scoring approaches and expert systems in structure-based virtual screening, Curr. Opin. Chem. Biol. 8 (2004) 359–364.

[19] S. Grüneberg, M.T. Stubbs, G. Klebe, Successful virtual screening for novel inhibitors of human carbonic anhydrase: strategy and experimental confirmation, J. Med. Chem. 45 (2002) 3588–3602.

[20] J. Wang, X. Kang, I.D. Kuntz, P.A. Kollman, Hierarchical database screenings for HIV-1 reverse transcriptase using a pharmacophore model, rigid docking, solvation docking, and MM-PB/SA, J. Med. Chem. 48 (2005) 2432–2444.

[21] E. Perola, Minimizing false positives in kinase virtual screens, Proteins: Struct. Funct. Bioinform. 64 (2006) 422–435.

[22] T.M. Steindl, D. Schuster, G. Wolber, C. Laggner, T. Langer, High-throughput structure-based pharmacophore modelling as a basis for successful parallel virtual screening, J. Comput. Aid. Mol. Des. 20 (2006) 703–715.

[23] N. Bharatham, K. Bharatham, Lee.F K.W., Pharmacophore identification and virtual screening for methionyl-tRNA synthetase inhibitors, J. Mol. Graph. Model. 25 (2007) 813–823.

[24] B. Gopalakrishnan, V. Aparna, J. Jeevan, M. Ravi, G.R. Desiraju, A virtual screening approach for thymidine monophosphate kinase inhibitors as antitubercular agents based on docking and pharmacophore models, J. Chem. Inf. Mod. 45 (2005) 1101–1108.

[25] H. Claussen, M. Gastreich, V. Apelt, J. Greene, S.A. Hindle, C. Lemmen, The FlexX database docking environment–rational extraction of receptor based pharmacophores, Curr. Drug Discov. Technol. 1 (2004) 49–60.

[26] A.C. Good, D.L. Cheney, D.F. Sitkoff, J.S. Tokarski, T.R. Stouch, D.A. Bassolino, S.R. Krystek, Y. Li, J.S. Mason, T.D.J. Perkins, Analysis and optimization of structure-based virtual screening protocols 2. Examination of docked ligand orientation sampling methodology: mapping a pharmacophore for success, J. Mol. Graph. Model. 22 (2003) 31–40.

[27] X. Fradera, R.M.A. Knegtel, J. Mestres, Similarity-driven flexible ligand docking, Proteins: Struct. Funct. Bioinform. 40 (2000) 623–636.

[28] S.A. Hindle, M. Rarey, C. Buning, T. Lengauer, Flexible docking under pharmacophore type constraints, J. Comput. Aid. Mol. Des. 16 (2002) 129–149.

[29] G. Klebe, Virtual ligand screening: strategies, perspectives and limitations, Drug Discov. Today 11 (2006) 580–594.

[30] C. McMartin, R.S. Bohacek, QXP: powerful, rapid computer algorithms for structure-based drug design, J. Comput. Aid. Mol. Des. 11 (1997) 333–344.

[31] A.N. Jain, Surflex: fully automatic flexible molecular docking using a molecular similarity-based search engine, J. Med. Chem. 46 (2003) 499–511.

[32] FRED 2.1.1, OpenEye Scientific Software, Santa Fe, USA.

[33] J.F. Beattie, G.A. Breault, R.P.A. Ellston, S. Green, P.J. Jewsbury, C.J. Midgley, R.T. Naven, C.A. Minshull, R.A. Pauptit, J.A. Tucker, J.E. Pease, Cyclin-dependent kinase 4 inhibitors as a treatment for cancer. Part 1. Identification and optimization of substituted 4,6-bis anilino pyrimidines, Bioorg. Med. Chem. Lett. 13 (2003) 2955–2960.

[34] R.G. Kurumbail, A.M. Stevens, J.K. Gierse, J.J. McDonald, R.A. Stegeman, J.Y. Pak, D. Gildehaus, J.M. Miyashiro, T.D. Penning, K. Seibert, P.C. Isakson, W.C. Stallings, Structural basis for selective inhibition of cyclooxygenase-2 by anti-inflammatory agents, Nature 384 (1996) 644–648.

[35] A.K. Shiau, D. Barstad, J.T. Radek, M.J. Meyers, K.W. Nettles, B.S. Katzenellenbogen, J.A. Katzenellenbogen, D.A. Agard, G.L. Greene, Structural characterization of a subtype-selective ligand reveals a novel mode of estrogen receptor antagonism, Nat. Struct. Biol. 9 (2002) 359–364.

[36] T. Matsusue, I. Shiromizu, A. Okamoto, K. Nakayama, H. Nishida, T. Mukaihira, Y. Miyazaki, F. Saitou, H. Morishita, S. Ohnishi, H. Mochizuki, Factor Xa specific inhibitor that induces the novel binding model in complex with human fXa. PDB release.

[37] A.G. Pavlovsky, M.G. Williams, Q.-Z. Ye, D.F. Ortwine, C.F. Purchase II, A.D. White, V. Dhanaraj, B.D. Roth, L.L. Johnson, D. Hupe, C. Humblet, T.L. Blundell, X-ray structure of human stromelysin catalytic domain complexed with nonpeptide inhibitors: implications for inhibitor selectivity, Protein Sci. 8 (1999) 1455–1462.

[38] B.J. Smith, P.M. Colman, M. Von Itzstein, B. Danylec, J.N. Varghese, Analysis of inhibitor binding in influenza virus neuraminidase, Protein Sci. 10 (2001) 689–696.

[39] H.M. Berman, J. Westbrook, Z. Feng, G. Gilliland, T.N. Bhat, H. Weissig, I.N. Shindyalov, P.E. Bourne, The protein data bank, Nucleic Acids Res. 28 (2000) 235–242.

[40] M. Jacobsson, A. Karlén, Ligand bias of scoring functions in structure-based virtual screening, J. Chem. Inf. Mod. 46 (2006) 1334–1343.

[41] R.D. Clark, Boosted leave-many-out cross-validation: the effect of training and test set diversity on PLS statistics, J. Comput. Aid. Mol. Des. 17 (2003) 265–275.

[42] Y. Tominaga, W.L. Jorgensen, General model for estimation of the inhibition of protein kinases using Monte Carlo simulations, J. Med. Chem. 47 (2004) 2534–2549.

[43] X. Yi, Z. Guo, F.M. Chu, Study on molecular mechanism and 3D-QSAR of influenza neuraminidase inhibitors, Bioorg. Med. Chem. 11 (2003) 1465–1474.
[44] H. Matter, E. Defossa, U. Heinelt, P.-M. Blohm, D. Schneider, A. Mueller, S. Herok, H. Schreuder, A. Liesum, V. Brachvogel, P. Loenze, A. Walser, F. Al-Obeidi, P. Wildgoose, Design and quantitative structure-activity relationship of 3-amidinobenzyl-1H-indole-2-carboxamides as potent, nonchiral, and selective inhibitors of blood coagulation factor Xa, J. Med. Chem. 45 (2002) 2749–2769.
[45] W. Sippl, Receptor-based 3D QSAR analysis of estrogen receptor ligands merging the accuracy of receptor-based alignments with the computational efficiency of ligand-based methods, J. Comput. Aid. Mol. Des. 14 (2000) 559–572.
[46] S. Ha, R. Andreani, A. Robbins, I. Muegge, Evaluation of docking/scoring approaches: a comparative study based on MMP3 inhibitors, J. Comput. Aid. Mol. Des. 14 (2000) 435–448.
[47] L.M. Shi, H. Fang, W. Tong, J. Wu, R. Perkins, R.M. Blair, W.S. Branham, S.L. Dial, C.L. Moland, D.M. Sheehan, QSAR models using a large diverse set of estrogens, J. Chem. Inf. Comput. Sci. 41 (2001) 186–195.
[48] G.E. Terp, B.N. Johansen, I.T. Christensen, F.S. Jorgensen, A new concept for multidimensional selection of ligand conformations (MultiSelect) and multidimensional scoring (MultiScore) of protein-ligand binding affinities, J. Med. Chem. 44 (2001) 2333–2343.
[49] C.A. Lipinski, F. Lombardo, B.W. Dominy, P.J. Feeney, Experimental and computational approaches to estimate solubility and permeability in drug discovery and development settings, Adv. Drug Deliv. Rev. 23 (1997) 3–25.
[50] Ligprep, Schrödinger LLC, New York.
[51] W.L. Jorgensen, D.S. Maxwell, J. Tirado-Rives, Development and testing of the OPLS all-atom force field on conformational energetics and properties of organic liquids, J. Am. Chem. Soc. 118 (1996) 11225–11236.
[52] SYBYL, 7.0, Tripos Inc., St. Louis.
[53] OMEGA, 1.8.1, OpenEye Scientific Software, Santa Fe.
[54] W. Welch, J. Ruppert, A.N. Jain, Hammerhead: fast, fully automated docking of flexible ligands to protein binding sites, Chem. Biol. 3 (1996) 449–462.
[55] J. Boström, J.R. Greenwood, J. Gottfries, Assessing the performance of OMEGA with respect to retrieving bioactive conformations, J. Mol. Graph. Model. 21 (2003) 449–462.
[56] M. Stahl, M. Rarey, Detailed analysis of scoring functions for virtual screening, J. Med. Chem. 44 (2001) 1035–1042.
[57] P. Gund, Three-dimensional pharmacophoric pattern searching, Prog. Mol. Subcell. Biol. 5 (1977) 117–143.
[58] UNITY, for SYBYL v.7.0, Tripos Inc., St. Louis.
[59] N. Triballeau, F. Acher, I. Brabet, J.-P. Pin, H.-O. Bertrand, Virtual screening workflow development guided by the ''Receiver Operating Characteristic'' curve approach. Application to high-throughput docking on metabotropic glutamate receptor subtype 4, J. Med. Chem. 48 (2005) 2534–2547.
[60] SIMCA-P+, 11.0, Umetrics AB, Umeå, Sweden.
[61] S. Maignan, J.-P. Guilloteau, Y.M. Choi-Sledeski, M.R. Becker, W.R. Ewing, H.W. Pauls, A.P. Spada, V. Mikol, Molecular structures of human factor Xa complexed with ketopiperazine inhibitors: preference for a neutral group in the S1 pocket, J. Med. Chem. 46 (2003) 685–690.
[62] M. Jacobsson, P. Liden, E. Stjernschantz, H. Boström, U. Norinder, Improving structure-based virtual screening by multivariate analysis of scoring data, J. Med. Chem. 46 (2003) 5781–5789.
[63] R.C. Wade, Flu'' And structure-based drug design, Structure 5 (1997) 1139–1145.